# Magnetic resonance elastography in the brain: an in silico study on the influence of cranial anatomy

Deirdre M McGrath[1,2], Nishant Ravikumar[1], Alejandro F Frangi[1], Iain D Wilkinson[2], and Zeike A Taylor[1]

[1]*CISTIB, Center for Computational Imaging & Simulation Technologies in Biomedicine, University of Sheffield, Sheffield, South Yorkshire, United Kingdom,* [2]*Academic Radiology, University of Sheffield, Sheffield, South Yorkshire, United Kingdom*

**TARGET AUDIENCE:** Magnetic resonance elastography researchers developing methodology for brain.

**PURPOSE:** Magnetic resonance elastography (MRE) of the brain is currently being evaluated as a biomarker of neurodegenerative disease such as dementia[1,2]. As MRE-measured biomechanical data for healthy brain varies widely[3], it is important to assess the possible impact of factors such as variable brain geometry and cranial anatomy. Recent work has suggested that the processes of the *dura mater* - the *falx cerebri* and *tentorium cerebelli* membranes - play a role in wave transmission through reflection or vibration[4]. As calcification of the *falx cerebri* can occur with aging[5], the influence of this structure may vary with age. 3D finite element model (FEM) simulations are presented for brain models to explore the sensitivity of MRE displacement fields and inversion reconstructions to brain geometry, and reflections and wave interference from anatomical features.

**METHODS:** MRE was simulated using Abaqus v6.12 (Dassault Systèmes Simulia Corp, Providence, RI) direct-solution steady-state dynamic analysis at frequencies previously employed for brain MRE (Table 1). Meshing with linear tetrahedral hybrid (for near-incompressible material) elements (inter-node spacing ~0.7 mm) was carried out on brain shapes generated from MRI T1-weighted acquisitions of 5 healthy volunteers from a public database (brain-development.org*). These included sub-meshes for the whole brain, the *falx cerebri*, *tentorium* and *falx cerebelli* (FTM) the ventricles and the outer meningeal layer containing cerebral spinal fluid (CSF). Wave transmission from the skull to the brain occurs via a combination of mechanical vibration of the meninges, and acoustic wave propagation through the CSF. To simplify the problem of simulating wave delivery, the mechanical waves were simulated as beginning at the brain surface. The boundary conditions were harmonic displacement of 30μm amplitude in the head-foot direction to nodes on the outer brain surface. The displacements on the outer CSF nodes were fixed to zero to prevent wave energy reflecting back into the brain. The outer nodes of the FTM were added to the displacement node set to simulate additional wave delivery via these structures. The brain was modelled as a uniform isotropic viscoelastic medium with properties set to those measured by MRE for healthy brain[6,7] (Table 1), with Poisson's ratio = 0.499. The CSF of the outer meningeal layer and the ventricles were modelled as a soft viscoelastic solid[8], and the FTM modelled as an elastic solid[8] (Table 1). In order to examine the influence of the FTM a second set of simulations was carried out with the FTM set to brain material properties. The FEM calculation produced complex steady state displacement vectors ($\vec{u}$) for the nodes which were interpolated onto a cubic grid with a resolution of 3mm, i.e., simulating an MRE acquisition with isotropic 3-mm voxels. To solve for the biomechanical properties, direct inversion was employed according to methods outlined in Green *et al.*[7], solving the Navier-Stokes equation for the curl of the displacement field (divergence-free), thereby removing the contribution of the compressional wave component. For the steady state this reduces to inverting $-\rho\omega^2\vec{c} = \mu\nabla^2\vec{c} + i\omega\zeta\nabla^2\vec{c}$, where $\vec{c} = \nabla \times \vec{u}$, to solve for the shear modulus (μ) and the shear viscosity (ζ) at the given frequency (ω) for an assumed density (ρ), i.e., brain density approximated to that of water. The curl field was smoothed with a 3x3x3 box filter before calculation of the Laplacian, to reduce noise from the numerical approximations in the FEM and interpolation. Reconstructions of Storage (G′=μ) and Loss (G″=ωζ) moduli were calculated for the brain tissue and compared with ground truth.

| Brain material properties | | |
|---|---|---|
| Frequency (Hz) | G' (Pa) | G'' (Pa) |
| 25 | 1110 | 480 |
| 37.5 | 1310 | 570 |
| 50 | 1520 | 600 |
| 62.5 | 2010 | 800 |
| 90 | 3100 | 2500 |
| **CSF material properties** | | |
| $G_0$ (Pa) | $G_\infty$(Pa) | β (s$^{-1}$) | K (MPa) |
| 1000 | 900 | 80 | 1050 |
| **FTM material properties** | | |
| E (MPa) | Poisson's ratio | |
| 31.5 | 0.45 | |

Table 1: FEM simulation material properties

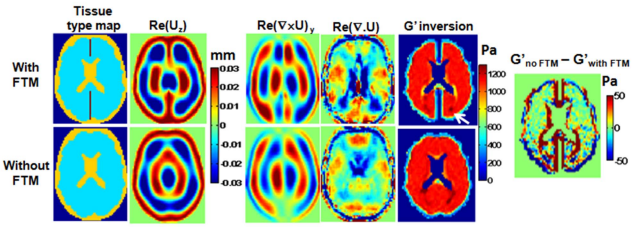


Figure 1: Top row: with FTM, lower row: without FTM. Left to right: tissue type maps, Re(U$_z$) at 25 Hz, Re(∇×U)$_y$, Re(∇.U), G' inversion maps, G'$_{no\ FTM}$ – G'$_{with\ FTM}$

**RESULTS:** Fig. 1 compares an example slice through the simulated brain volume with and without the FTM and demonstrates how the displacements, curl and divergence (Re($u_z$), Re(∇×u)$_y$, and Re(∇.u)) and the G' inversion maps are strongly influenced by the presence of the FTM. The divergence plot with FTM indicates the location of the *falx* as a source of wave excitation. Some large inversion artefacts (white arrow) were present on the G' maps and these varied in shape with and without the FTM. The difference map of the G' maps shows some large variations, in particular in the corners between the *falx* and the ventricles. Fig.2 plots mean(±std) parameters for the 5 brain meshes with and without FTM. Fig. 2a plots the mean displacement vector magnitude over the brain volume against MRE frequency, and this reduces with frequency, i.e., more rapid wave attenuation in viscoelastic brain at higher frequencies. However it increases with the inclusion of the FTM, suggesting transmission and/or reflection of wave energy from the FTM. Re(∇×u)$_y$ (Fig. 2b) increases and then decreases with frequency, which may be explained by the initial benefit of shorter wavelengths at higher frequencies implying a larger value of curl, followed by an overall reduction in displacement magnitude and curl because of attenuation; but it is always larger with the FTM. The mean % error in G' (100×(inversion G' – ground truth G')/ ground truth G') (Fig. 2c) is a combination of edge artefacts due to reflections and interactions at the various tissue interfaces, along with the influence of the 3$^{rd}$ order derivatives and smoothing of the curl field at brain edges. The error reduces with increasing frequency, which may possibly be explained by higher curl values at higher frequencies, but also by different interactions and reflections from tissue interfaces. With the FTM, at lower frequencies the error is worse but improves with increasing frequency. The mean % error in G'' is also frequency dependent, with an initial increase in magnitude, followed by a decrease; and the error magnitude is larger with the FTM. The errors are predominantly associated with edge effects, as when the brain volume mask is eroded by a layer 3 voxels wide, the mean error magnitude is reduced to <3% in G' and <0.5% in G''. Importantly, the parameters showed variation across the 5 brain meshes, demonstrating a sensitivity to individual anatomy.

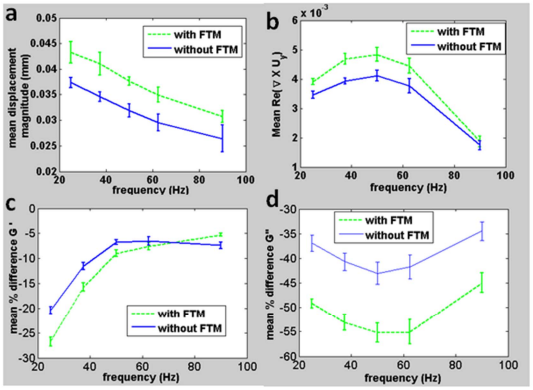


Figure 2: Mean (± std) data for brain tissue from 5 brain meshes vs. MRE frequency, with and without falx and tentorium: (a) mean displacement magnitude, (b) Mean magnitude of (∇× U)$_y$, (c) mean % difference G', (d) mean % difference G''

**DISCUSSION:** Acoustic waves reflect at tissue boundaries according to the relative mismatch of acoustic impedance between the tissue types, which is dependent on the elastic modulus and density. The material properties employed in this study could imply over 90% reflection of incident waves at a brain-*falx* boundary and 30% at the brain-CSF boundary. The interactions between the waves scattered from multiple interfaces may result in interference and standing wave patterns, which confound accurate estimates of G' and G''. Errors were more likely at lower frequencies and in particular where there are multiple neighbouring reflective interfaces. These effects are likely to be important given that initial MRE data for Alzheimer's disease[1] reports decreases of less than 1kPa in G' from control to patient groups and an MRE ageing study[6] reported a decrease in G' of less than 10 Pa per year.

**CONCLUSION:** These simulations indicate that the structures of the *falx cerebri*, *tentorium cerebelli*, and the ventricles have an important influence on the displacement fields generated in the brain during MRE and the resulting inversion maps. However further work is required to understand the implications of these findings *in vivo*, and, in particular, through comparison with acquired MRE data.

**References:** **[1]** *Murphy, M.C., et al., J Magn Reson Im 2011. 34: p. 494-498*; **[2]** *Lipp, A., et al., Neuroimage Clin, 2013; 3: p. 381-7;* **[3]** *Di Leva, A., et al., Neurosurg Rev, 2010. 33(2): p. 137-45; discussion 145;* **[4]** *Clayton, E.H., et al., J R Soc Interface, 2012. 9(76): p. 2899-910;* **[5]** *Daghighi, M.H., et al., Folia Morphol (Warsz), 2007. 66(2): p. 115-9;* **[6]** *Sack, I., et al., Neuroimage, 2009. 46(3): p. 652-7.;* **[7]** *Green, M.A. et al., NMR Biomed, 2008. 21(7): p. 755-64;* **[8]** *Wittek et al 2011, Computational Biomechanics for Medicine, Soft Tissues and the Muskoloskeletal System, Springer.* 